

Quantum coherence in semiconductor superlattices

F. Agulló-Rueda,* E. E. Mendez, and J. M. Hong

IBM Research Division, Thomas J. Watson Research Center, P. O. Box 218, Yorktown Heights, New York 10598

(Received 26 April 1989; revised manuscript received 22 May 1989)

Using photocurrent spectroscopy, we have demonstrated that the quantum coherence in GaAs-Ga_{1-x}Al_xAs superlattices increases with decreasing superlattice period D , and that it is maintained for at least ten periods when $D=60$ Å. The coherence length was determined from the number of observed interband transitions between the valence- and conduction-band Stark ladders, formed when an electric field was applied along the superlattice direction. As an additional manifestation of the Stark ladder, the photocurrent showed strong oscillations, periodic in the reciprocal of the electric field, which gave rise to regions of pronounced negative differential resistance.

In an ideal superlattice, consisting of a periodic repetition of quantum wells separated by narrow potential barriers, the electronic states are completely delocalized and their energies are distributed in minibands that result from the strong coupling among the wells. In a real superlattice, however, deviations from perfect periodicity caused, e.g., by well-width or barrier-height fluctuations, reduce the coupling and induce a degree of localization thus decreasing the coherence length of the superlattice wave functions. Under strong localization coherence will be reduced to a few periods and in the limit, to a single quantum well.

Since the existence of wave-function coherence is essential to the realization of devices that exploit the superlattice concept, a determination of that physical quantity and an understanding of the parameters that affect it are of paramount importance. Recently, we have directly observed the formation of Stark ladders in semiconductor superlattices under electric fields and demonstrated the possibility of using interband transitions between Stark-ladder states to determine the quantum coherence λ of the superlattice wave functions.¹ Here we exploit this technique to show experimentally that λ increases as the superlattice period D decreases, becoming at least ten-period long when $D=60$ Å.

The coupling between wells decreases when an electric field \mathcal{E} is applied along the superlattice direction because the field shifts the states of each well. Thus, the net effect of the field is similar to that of disorder in that it reduces the electronic coherence. Extreme localization occurs at very high fields, with the quantum states confined to individual wells. Simultaneously, a miniband of energy width Δ splits into a series of discrete levels (Stark-ladder levels), whose wave functions are centered in individual wells but extending to neighboring ones.²⁻⁵ The energies of interband transitions between conduction- and valence-band Stark states of indices n and m , respectively, are given by¹

$$E_{nm}(\mathcal{E}) = E_0(\mathcal{E}) + (n-m)e\mathcal{E}D \quad (n, m = 0, \pm 1, \pm 2, \dots), \quad (1)$$

where E_0 is the intrawell ($n-m=0$) transition energy in the isolated-well limit. Since the strength of a transition

between two states is proportional to the overlap between the corresponding hole and electron wave functions, for a given \mathcal{E} the intensities of interwell transitions ($n-m \neq 0$) will decrease rapidly with increasing index $\nu = |n-m|$, and the number of optical transitions observed experimentally will be a measure of the combined extension of the wave functions. Because of their large effective mass, heavy-hole states are coupled weakly and become fully localized under rather small fields. Thus, in practice, the number of interwell transitions involving heavy holes measures directly the spatial extent of the electron wave functions, and a zero-field extrapolation will give the maximum coherence length of the electronic states.

In our study, a set of superlattices were formed by sixty periods of alternating GaAs and Ga_{0.65}Al_{0.35}As layers, terminated by 600 Å of Ga_{0.65}Al_{0.35}As on each side. These undoped structures constituted the intrinsic regions of p^+i-n^+ diodes grown by molecular-beam epitaxy, in which the well (barrier) thicknesses of the superlattices were 40(20), 30(35), 40(30), 40(35), 40(40), and 50(35) Å. An external voltage V on the p^+ region (relative to the n^+ side) produced a very uniform electric field in the superlattice, which to first approximation was given by $\mathcal{E} \approx |V - V_b|/W$, where V_b is the built-in voltage ($V_b \approx 1.55$ V), and W is the thickness of the intrinsic region. A more accurate relation between V and \mathcal{E} was obtained from a determination of the potential profile by numerical integration of Poisson's equation, which showed the validity of the above approximation.

Photocurrent (PC) spectra in the temperature range 5–200 K were measured at various voltages using low-power excitation (<0.2 W/cm²) from a dye laser pumped by a Kr⁺ laser. Similarly, photoluminescence emission and excitation spectra were recorded with a GaAs photomultiplier at the exit slit of a doublepass, 0.85-m focal length, monochromator. Except at very low electric fields, the photocurrent had much better signal-to-noise ratio than the photoluminescence whose intensity decreased rapidly with increasing field. Moreover, being proportional to the optical absorption, the photocurrent is easier to interpret than luminescence. Here we will focus on the PC measurements and will postpone a comparison with photoluminescence results to a future publication.

Selected spectra near the fundamental gap for the 60-Å-period superlattice are given in Fig. 1 at various electric fields between 5.6 and 167 kV/cm. As \mathcal{E} increases, the PC spectra experience drastic changes, evolving from simple to complex and then to simple again at the highest fields when only two structures remain. This behavior was independent of temperature, with the same number of features present even at 200 K, although somewhat broader than at low T .

The PC peaks reflect the excitonic nature of the interband optical transitions between the valence and conduction bands of the superlattice. Their energy variation with electric field, which is obtained from a complete set of spectra like those of Fig. 1, and from measurements of the photocurrent-versus-voltage characteristics at fixed laser energy (see below), is depicted in Fig. 2 where, for clarity, we have separately plotted the heavy-hole and the light-hole transitions. These results can be more easily analyzed if we distinguish three situations according to the effect of the field on the electron and light-hole bands: the "miniband," the Stark ladder, and the multiquantum-well regimes. (In practice, the heavy holes are localized even at the lowest fields.)

Although strictly speaking, a miniband is broken into Stark levels even for very small fields, if their separation is small compared to the intrinsic broadening, δ (caused, e.g., by thickness fluctuations along the plane of the wells), the Stark levels are unresolved. Then, it is still possible to consider a miniband regime where the photocurrent (see Fig. 1) resembles the absorption spectrum of a superlattice at $\mathcal{E} = 0$, with two peaks (at 1.633 and 1.652

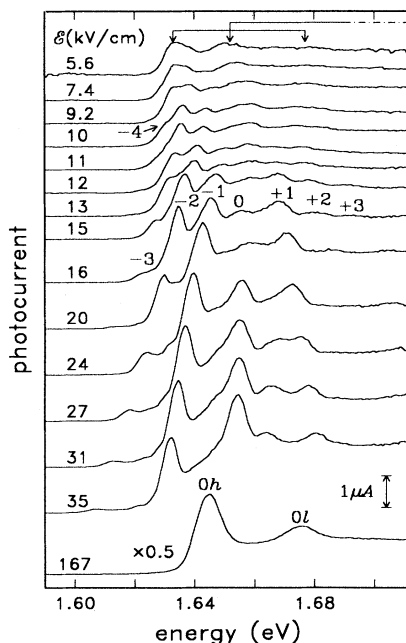


FIG. 1. Photocurrent spectra for the 60-Å-period superlattice at 5 K, for selected values of the electric field applied perpendicular to the layers. Spectra have been offset vertically for clarity. The peak labels at low field give the Stark ladder index ν of electrons for heavy-hole to conduction-band transitions.

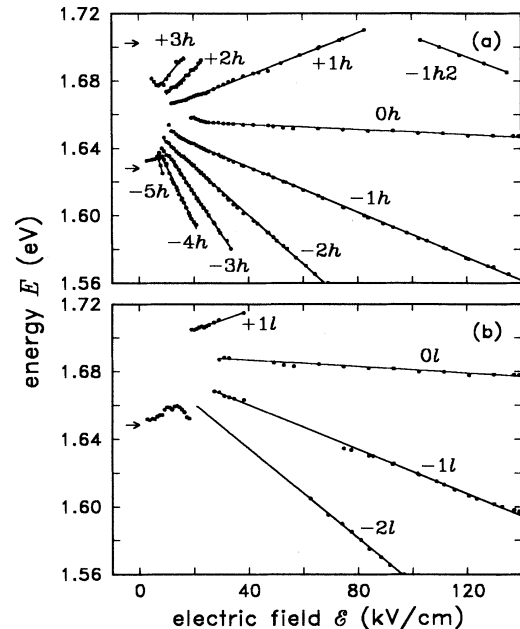


FIG. 2. Transition energies near the band gap as a function of the electric field for the 60-Å-period superlattice, obtained from photocurrent measurements at 5 K. Arrows give the transition energies at $\mathcal{E} = 0$ calculated with a Kronig-Penney model. (a) Heavy hole to conduction band. (b) Light hole to conduction band. Straight lines are least-squares fits to the experimental points.

eV for $\mathcal{E} = 5.6$ kV/cm) corresponding to the onset of the heavy- and light-hole transitions to the bottom of the electron miniband, respectively. A third weak feature (at 1.677 eV for $\mathcal{E} = 5.6$ kV/cm) arises from the heavy-hole transition to the top of the electron miniband.

This identification is consistent with a Kronig-Penney band calculation at zero field,⁶ which predicts energy bandwidths of 70, 4, and 58 meV, for electrons, heavy holes, and light holes, respectively. The calculated energies of the optical transitions are shown by small arrows in Fig. 2. (The transition involving the top of the light-hole and electron minibands was outside the spectral range of the dye laser.) For increasing electric fields, and before they effectively split into Stark ladders, the minibands get narrower (see Fig. 2) as the number of wells that contribute to the superlattice states decreases. The observed narrowing is asymmetric, with a faster shift of the higher edge of the miniband, as expected from a reduction of well coupling.

At moderate fields ($\delta \leq e\mathcal{E}D < \Delta$), the minibands are broken into a series of discrete states, and we enter the Stark-ladder regime with electronic wave functions extending over a few superlattice periods. The labels in Fig. 2(a) correspond to the Stark-ladder indices for electrons, ranging from -5 to $+3$. As Fig. 2 shows, in this regime the energies vary linearly with the electric field. Moreover, the period can be estimated from the difference in slope between interwell and intrawell transitions. A least-squares fit to these differences, plotted in Fig. 3(a) versus their Stark indices, yields an estimation for D that

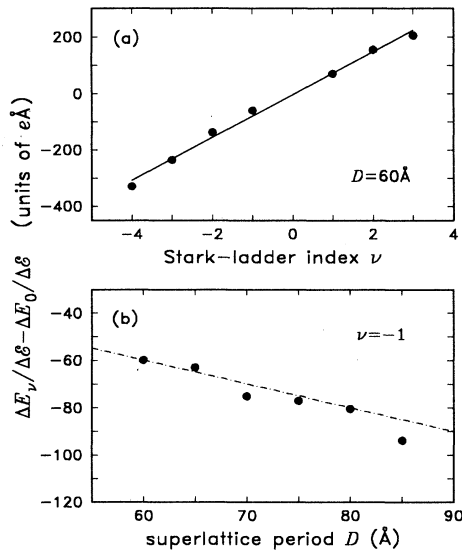


FIG. 3. (a) Slopes obtained from the fits in Fig. 2(a) as a function of the Stark ladder index. The solid line is a fit to the points. (b) The slope of the $(-1h)$ transition for different samples as a function of the superlattice period. The dashed line gives the theoretical dependence $\epsilon\nu D$. To account for the field dependence of E_{0h} in both (a) and (b) the slopes have been subtracted by the slope of the $(0h)$ transition.

agrees to within 20% of the nominal period. The discrepancy arises probably from the inaccuracy in the slopes of the high-index transitions, the excitonic effects [not included in Eq. (1)], and the error in the actual period.

The observation of up to nine different transitions ($\nu = -5, -4, \dots, +2, +3$) in Fig. 2(a) and even of a tenth one ($\nu = -6$) at very low fields (see Fig. 4), gives a lower bound of ten periods for the coherence length of the superlattice at $\mathcal{E} = 0$. Actually, the expected symmetry of the Stark ladder implies a minimum coherence of thirteen wells, from $\nu = -6$ to $\nu = +6$ although the $\nu = +4, +5, +6$ transitions were not observed. This long coherence decreases when the period of the superlattice increases, as similar PC measurements in samples with $60\text{\AA} < D < 85\text{\AA}$ demonstrate. Indeed, for the superlattice with the largest period, only the $\nu = 0$ and -1 transitions were observed, an indication of a coherence of only two periods. The unexplained absence of the $\nu = +1$ transition in this case is consistent with the asymmetry observed in all samples: The transitions with $\nu > 0$ are always weaker than their counterparts with $\nu < 0$. In Fig. 3(b) we represent the slopes for the $\nu = -1$ transition as a function of the period, which increase linearly with D , in agreement with the prediction of Eq. (1), as shown by the dashed line.

Although for simplicity the above analysis has been focused on the heavy-hole transitions, similar conclusions can be drawn from those involving light holes, regardless of their partial delocalization. An additional transition, involving a heavy-hole level above the ground state and labeled $-1h_2$ in Fig. 2(a), is observed in the PC spectra. It

corresponds to a forbidden (in the $\mathcal{E} = 0$ limit) transition from the second heavy-hole level to the electron Stark level $\nu = -1$ and behaves similarly to the fundamental transition $-1h$.

In the multi-quantum-well regime, when $\Delta \ll \epsilon \mathcal{E} D$, only the intrawell transitions $0h$ and $0l$ remain visible in the PC spectra, once the wells become effectively uncoupled. As observed in Fig. 2, the energies of both transitions decrease as \mathcal{E} increases, the shift reaching up to ≈ 20 meV for heavy-hole transitions at the highest field of 250 kV/cm. The main cause of these shifts are as follows: the Stark effect in individual wells and the increase in exciton binding energy due to field-induced localization. The Stark shift (calculated using a transfer-matrix method⁷) for a single 40- \AA well is 13.8 meV (17.4 meV) for the heavy- (light-) hole to conduction-band transition, at $\mathcal{E} = 250$ kV/cm. The binding energy of the heavy-hole exciton increases from ≈ 6 meV in the superlattice regime⁸ to about 13 meV in the high-field regime.⁹ The sum of these two contributions is very close to the measured shifts. A third effect of the electric field,¹⁰ much weaker and of opposite sign, is the slight reduction of the binding energy of the exciton once it is localized in an isolated well.

The transition from a quasi-three-dimensional (superlattice) to a quasi-two-dimensional (quantum-well) exciton was clearly visible in the energy difference between the exciton peak and the onset of the band-to-band transition that gives a drastic increase in the exciton binding energy. This behavior also produces the rapid energy decrease of $0h$ at around 30 kV/cm seen in Fig. 2(a). A detailed account of these results will be given elsewhere.

Finally, let us consider another manifestation of the Stark ladder in the form of negative differential resistance features in the photocurrent, as seen in Fig. 4 for the superlattice with $D = 60\text{\AA}$. The peaks in the photocurrent-voltage (PCV) characteristic correspond to maxima in the absorption coefficient whenever the energy separation between valence- and conduction-band Stark states coincides with the incident photon energy. The inset of Fig. 4,

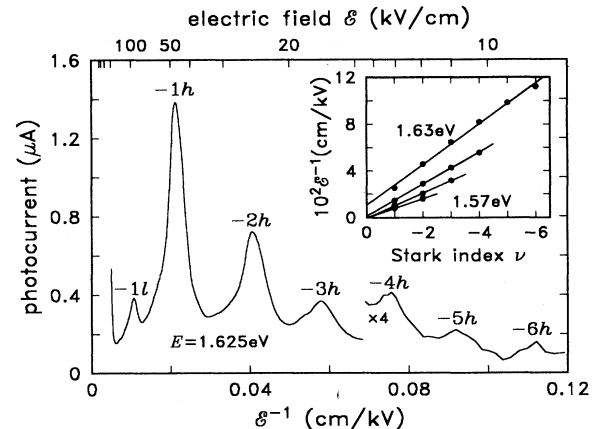


FIG. 4. Photocurrent characteristic for the 60- \AA -period superlattice measured as a function of the electric field at a laser energy of 1.625 eV. The inset gives the position of the maxima of the oscillations for heavy holes vs the Stark-ladder index ν , obtained for different laser energies separated by 20 meV.

plotting the PC maxima for several excitation energies, demonstrates their periodicity with \mathcal{E}^{-1} . This is in agreement with the prediction of Eq. (1), which can be rewritten as $\nu = (E_\nu - E_0)\mathcal{E}_\nu^{-1}/eD$. The oscillations decay for high values of ν , as they represent transitions between very distant wells.

Similar to the structures of PC spectra, the number of Stark-ladder oscillations observed in a superlattice provide a direct measure of its electronic coherence. Moreover, the slightly higher sensitivity of the PCV characteristics allows the resolution of Stark-ladder levels up to $\nu = -6$. We note here the difference between these oscillations, periodic in \mathcal{E}^{-1} and observed in superlattices under excitation energies either below or above the fundamental band gap, and the Franz-Keldysh oscillations,¹¹ which are periodic in $\mathcal{E}^{2/3}$ and observable only for above band gap excitation.

In summary, we have demonstrated that a superlattice

parameter as fundamental as the electronic coherence increases as the period decreases and becomes at least ten periods long when $D = 60$ Å. This coherence is maintained at least up to 200 K, suggesting that it is not restricted by inelastic scattering with residual impurities. The actual limit may lie in small fluctuations in layer thickness or alloy composition. Optimization in the design and fabrication of these heterostructures will undoubtedly lead to even larger coherence lengths and bring closer to reality the properties of an ideal superlattice.

This work has been sponsored in part by the Army Research Office. F.A.-R. acknowledges the support of the Institute of Materials Science of Madrid (Spain). We thank L. L. Chang and J. A. Brum for valuable discussions, L. F. Alexander for sample preparation, and A. Warren for the computer program to calculate the potential distribution in the heterostructures.

*Permanent address: Instituto de Ciencia de Materiales, Consejo Superior de Investigaciones Científicas, Universidad Autónoma, Cantoblanco, E-28049 Madrid, Spain.

¹E. E. Mendez, F. Agulló-Rueda, and J. M. Hong, *Phys. Rev. Lett.* **60**, 2426 (1988).

²P. W. A. McClroy, *J. Appl. Phys.* **59**, 3532 (1986).

³E. Cota, J. V. José, and G. Monsiváis, *Phys. Rev. B* **35**, 8929 (1987).

⁴C. F. Hart, *Phys. Rev. B* **38**, 2158 (1988).

⁵J. Bleuse, G. Bastard, and P. Voisin, *Phys. Rev. Lett.* **60**, 220 (1988).

⁶The parameters used in the calculations were 0.308 eV (0.189 eV) for the conduction- (valence-) band barrier heights, and

0.0665(0.0895), 0.34(0.51), and 0.094(0.116) for the effective masses of electrons, heavy holes, and light holes in the well (barrier) in units of the free-electron mass.

⁷E. E. Mendez, in *Physics and Applications of Quantum Wells and Superlattices*, edited by E. E. Mendez and K. von Klitzing (Plenum, New York, 1988), p. 159.

⁸A. Chomette, B. Lambert, B. Deveaud, F. Clerot, A. Regreny, and G. Bastard, *Europhys. Lett.* **4**, 461 (1987).

⁹E. S. Koteles and J. Y. Chi, *Phys. Rev. B* **37**, 6332 (1988).

¹⁰J. A. Brum and G. Bastard, *Phys. Rev. B* **31**, 3893 (1985); S. Nojima, *ibid.* **37**, 9087 (1988).

¹¹F. Bassani and G. P. Parravicini, *Electronic States and Optical Transitions in Solids* (Pergamon, Oxford, 1975), p. 267.